Cluster Dynamical Mean Field Theory with an ED Solver

David Sénéchal

Département de physique & Institut Quantique
Université de Sherbrooke

International Summer School on Computational Quantum Materials
May 27, 2024

Outline

1. Cluster Dynamical Mean Field Theory
2. The impurity solver: Exact Diagonalizations
3. Application to the Emery model
4. PyQCM : a python library for CPT, CDMFT and VCA
5. Advert

Outline

1 Cluster Dynamical Mean Field Theory
- The hybridization function
- The CDMFT self-consistency condition
- Applications
- Superconductivity

2 The impurity solver: Exact Diagonalizations

3 Application to the Emery model

4 PyQCM : a python library for CPT, CDMFT and VCA

5 Advert

Why clusters?

- To capture short-range fluctuations exactly.
- Important for effective (non-Hubbard) interactions mediated by short-range fluctuations
- $\longrightarrow$ Superconductivity!
- The computational cost quickly rises with cluster size
- Two paradigms:
  - Cluster (or Cellular) Dynamical Mean Field Theory (CDMFT) : real-space based

    Lichtenstein et al, PRB 62, R9283 (2000); Kotliar et al, PRL 87, 186401 (2001)
  - Dynamical Cluster Approximation (DCA) : momentum-space based

    Hettler et al, PRB 58, R7475 (1998)

Cluster kinematics

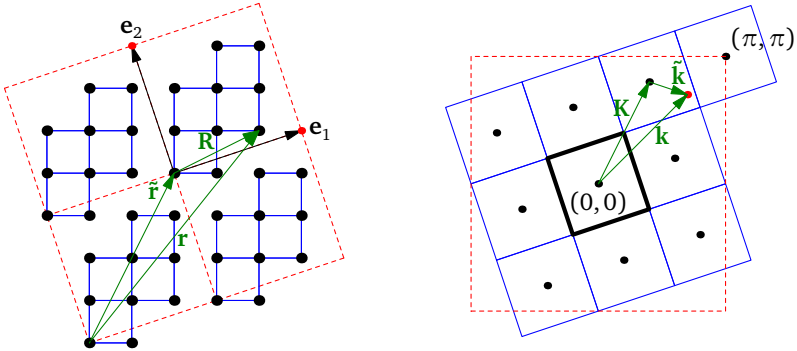

(a) (b)

- Periodization: Clustering breaks translation invariance, which needs to be restored:

$$\boxed{G_{\text{per.}}(\boldsymbol{k}, \omega) = \frac{1}{L} \sum_{\boldsymbol{R}, \boldsymbol{R}'} \mathrm{e}^{-i\boldsymbol{k}\cdot(\boldsymbol{R}-\boldsymbol{R}')} G_{\boldsymbol{R}\boldsymbol{R}'}(\tilde{\boldsymbol{k}}, \omega)}$$

Generalization of DMFT to small clusters

- $H_{\mathrm{AIM}} \to H_c$
- Simple adaptation of DMFT
- Scalar equations become matrix equations

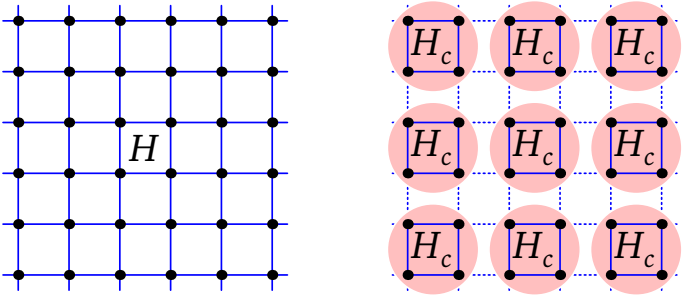

Dynamical mean field $\mathscr{G}_0$:

$$S_{\mathrm{eff}}[c, c^*] = -\int_0^\beta \mathrm{d}\tau \mathrm{d}\tau' \sum_{\alpha,\beta} c^*_\alpha(\tau) \mathscr{G}^{-1}_{0,\alpha\beta}(\tau - \tau') c_\beta(\tau') + \int_0^\beta \mathrm{d}\tau\, H_1(c, c^*)$$

The hybridization function

In the frequency domain:

hybridization function

$$\mathcal{G}_0^{-1}(i\omega_n) = i\omega_n - \boldsymbol{t}^c - \boldsymbol{\Gamma}(i\omega_n) \quad \text{where} \quad \mathcal{G}_0(i\omega_n) = \int_0^\beta \mathrm{e}^{i\omega_n\tau}\mathcal{G}_0(\tau)$$

Spectral representation of $\boldsymbol{\Gamma}$:

$$\Gamma_{\alpha\beta}(i\omega_n) = \sum_r^{N_b} \frac{\theta_{\alpha r}\theta^*_{\beta r}}{i\omega_n - \varepsilon_r} \quad \text{or} \quad \boldsymbol{\Gamma}(i\omega_n) = \boldsymbol{\theta}\frac{1}{i\omega_n - \boldsymbol{\varepsilon}}\boldsymbol{\theta}^\dagger$$

Can be represented in the Hamiltonian formalism by a set of noninteracting bath orbitals a_r:

hybridization matrix

bath orbital

$$H_c = \sum_{\alpha,\beta} t^c_{\alpha\beta} c^\dagger_\alpha c_\beta + U\sum_i n_{i\uparrow}n_{i\downarrow} + \sum_{r,\alpha}\theta_{r\alpha}(c^\dagger_\alpha a_r + \text{H.c.}) + \sum_r \varepsilon_r a^\dagger_r a_r$$

bath energies

The Anderson impurity model

Non interacting Green function (cluster+bath): $\boldsymbol{G}_0^{\text{full}}(\omega) = (\omega - \boldsymbol{T})^{-1}$

where $\boldsymbol{T} = \begin{pmatrix} \boldsymbol{t}^c & \boldsymbol{\theta} \\ \boldsymbol{\theta}^\dagger & \boldsymbol{\varepsilon} \end{pmatrix}$

$$\left(\boldsymbol{G}_0^{\text{full}}(\omega)\right)^{-1} = \begin{pmatrix} \omega - \boldsymbol{t}^c & -\boldsymbol{\theta} \\ -\boldsymbol{\theta}^\dagger & \omega - \boldsymbol{\varepsilon} \end{pmatrix} = \begin{pmatrix} A_{11} & A_{12} \\ A_{21} & A_{22} \end{pmatrix} = \begin{pmatrix} B_{11} & B_{12} \\ B_{21} & B_{22} \end{pmatrix}^{-1}$$

Need to extract the cluster component of $\boldsymbol{G}_0^{\text{full}}(\omega)$, i.e., B_{11}:

$$A_{11}B_{11} + A_{12}B_{21} = \mathbf{1} \qquad A_{21}B_{11} + A_{22}B_{21} = 0$$

$$B_{21} = -A_{22}^{-1}A_{21}B_{11} \implies \left(A_{11} - A_{12}A_{22}^{-1}A_{21}\right)B_{11} = \mathbf{1}$$

$$\boldsymbol{G}_{0c}^{-1} = \omega - \boldsymbol{t}^c - \boldsymbol{\Gamma}(\omega) \qquad \boldsymbol{\Gamma}(\omega) = \boldsymbol{\theta}\frac{1}{\omega - \boldsymbol{\varepsilon}}\boldsymbol{\theta}^\dagger$$

The Anderson impurity model (cont.)

Interacting case:
One must simply add the cluster self-energy $\boldsymbol{\Sigma}(\omega)$ (no self-energy on the bath).
The cluster Green function is then

$$\begin{aligned} \boldsymbol{G}_c^{-1}(\omega) &= \omega - \boldsymbol{t}^c - \boldsymbol{\Gamma}(\omega) - \boldsymbol{\Sigma}(\omega) \\ &= \mathscr{G}_0^{-1}(\omega) - \boldsymbol{\Sigma}(\omega) \end{aligned}$$

Discrete bath systems

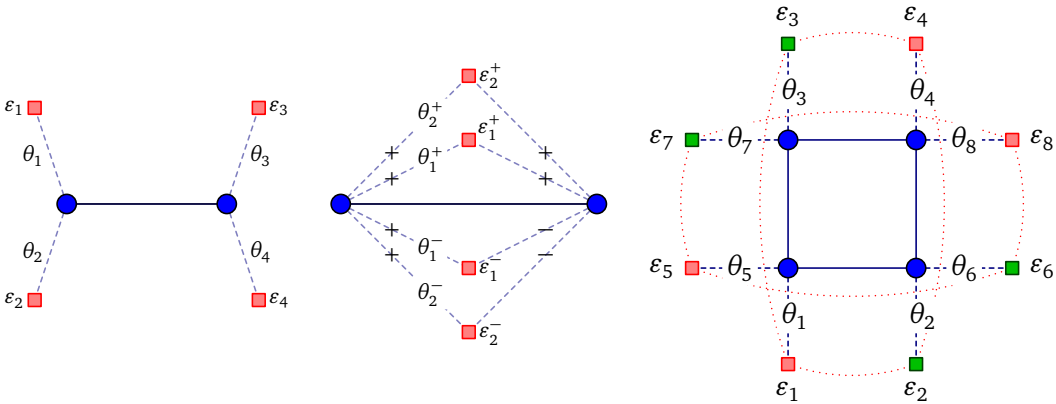

(A) (B) (C)

The CDMFT Procedure (discrete bath)

1. Start with a guess value of $(\theta_{\alpha r}, \varepsilon_r)$.
2. Calculate the cluster Green function $\boldsymbol{G}_c(\omega)$ (ED).
3. Calculate the superlattice-averaged Green function

$$\bar{\boldsymbol{G}}(\omega) = \sum_{\tilde{k}} \frac{1}{\boldsymbol{G}_0^{-1}(\tilde{\boldsymbol{k}}) - \boldsymbol{\Sigma}(\omega)}$$

4. Minimize the following distance function:

$$d(\boldsymbol{\theta}, \boldsymbol{\varepsilon}) = \sum_{\omega_n} W(i\omega_n) \operatorname{tr} \left| \boldsymbol{G}_c^{-1}(i\omega_n) - \bar{\boldsymbol{G}}^{-1}(i\omega_n) \right|^2$$

   over the set of bath parameters with fixed $\bar{\boldsymbol{G}}$. Thus obtain a new set $(\theta_{\alpha r}, \varepsilon_r)$.
5. Go back to step (2) until convergence.

The CDMFT self-consistency loop

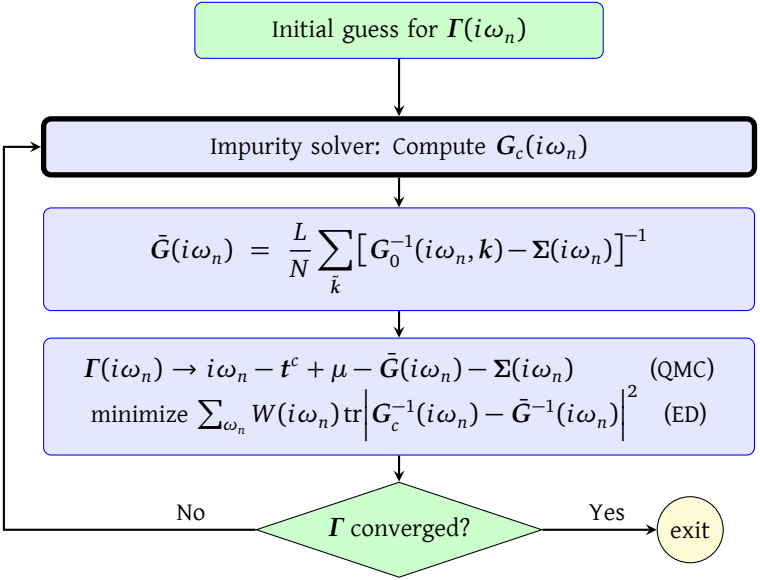

Discrete bath drawbacks (ED)

- The hybridization function has a finite number of poles.
- There is some arbitrariness in the choice of distance function.
- There is some arbitrariness in the choice of the bath configuration.
- Normal state: The number of electrons in the impurity is quantized; there are Hilbert space sectors and hence discontinuities as a function of chemical potential.
- ED : Zero temperature is not really zero! There is an effective energy scale $\sim$ level separation.

n vs μ in the 1D Hubbard model ($U = 4t$, $L = 4$, $n_b = 4$):

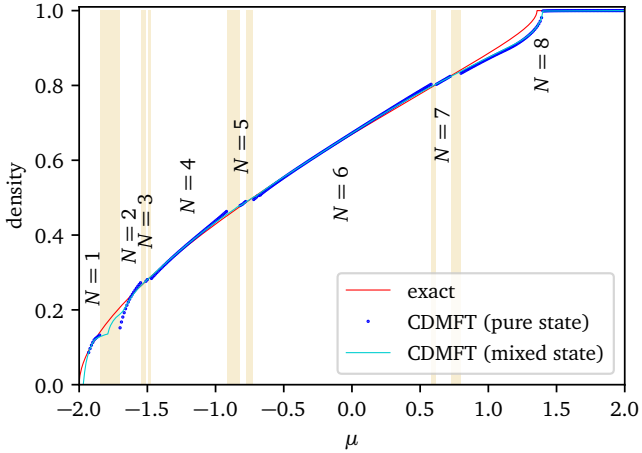

Application: The Mott transition

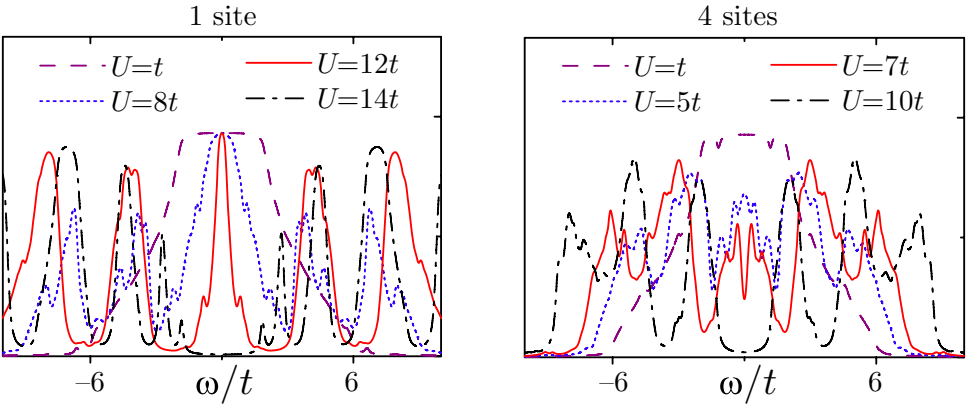

Y.Z. Zhang, M. Imada, Phys. Rev. B **76**, 045108 (2007)

Application: the Mott transition

QCM:

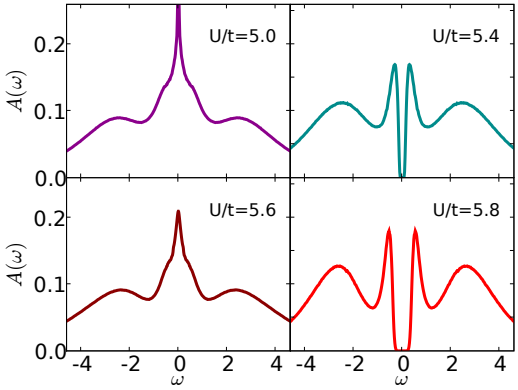

H. Park et al, PRL 101, 186403 (2008)

ED:

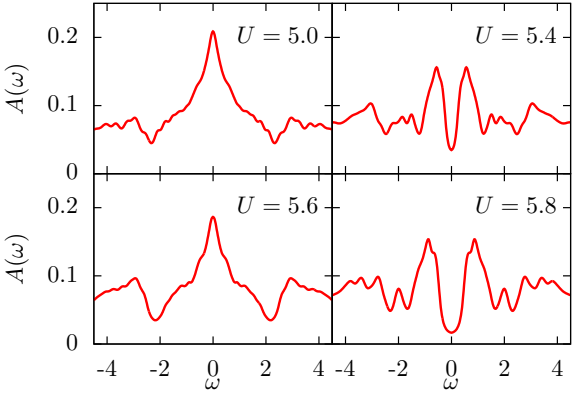

solutions from M. Balzer et al., Europhys. Lett. 85, 17002 (2009)

Pairing operators

- Superconductivity is described by pairing fields:

$$\Delta = \sum_{r,r'} \Delta_{rr'} c_{r\uparrow} c_{r'\downarrow} + \text{H.c}$$

- s-wave pairing: $\Delta_{rr'} = \delta_{rr'}$
- $d_{x^2-y^2}$ pairing:

$$\Delta_{rr'} = \begin{cases} 1 & \text{if} \quad \boldsymbol{r} - \boldsymbol{r}' = \pm \boldsymbol{x} \\ -1 & \text{if} \quad \boldsymbol{r} - \boldsymbol{r}' = \pm \boldsymbol{y} \end{cases}$$

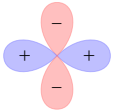

- d_{xy} pairing:

$$\Delta_{rr'} = \begin{cases} 1 & \text{if} \quad \boldsymbol{r} - \boldsymbol{r}' = \pm(\boldsymbol{x} + \boldsymbol{y}) \\ -1 & \text{if} \quad \boldsymbol{r} - \boldsymbol{r}' = \pm(\boldsymbol{x} - \boldsymbol{y}) \end{cases}$$

- Pairing fields are introduced in the bath, and measured on the cluster

Pairing operators (cont.)

- Pairing fields violate particle number conservation
- The Hilbert space is enlarged to encompass all particle numbers with a given total spin
- Use the **Nambu formalism**: a particle-hole transformation on the spin-down sector: $c_{\alpha\downarrow} \to c^\dagger_{\alpha\downarrow}$ and $a_{r\downarrow} \to a^\dagger_{r\downarrow}$
- Possible structures of the one-body matrix:

$$\begin{array}{c} c_\uparrow \\ a_\uparrow \\ c^\dagger_\downarrow \\ a^\dagger_\downarrow \end{array} \begin{pmatrix} \boldsymbol{t}_\uparrow & \boldsymbol{\theta}_\uparrow & 0 & 0 \\ \boldsymbol{\theta}^\dagger_\uparrow & \boldsymbol{\varepsilon}_\uparrow & 0 & \Delta_b \\ 0 & 0 & -\boldsymbol{t}_\downarrow & -\boldsymbol{\theta}_\downarrow \\ 0 & \Delta^\dagger_b & -\boldsymbol{\theta}^\dagger_\downarrow & -\boldsymbol{\varepsilon}_\downarrow \end{pmatrix} \quad \text{or} \quad \begin{array}{c} c_\uparrow \\ a_\uparrow \\ c^\dagger_\downarrow \\ a^\dagger_\downarrow \end{array} \begin{pmatrix} \boldsymbol{t}_\uparrow & \boldsymbol{\theta}_\uparrow & 0 & \Delta \\ \boldsymbol{\theta}^\dagger_\uparrow & \boldsymbol{\varepsilon}_\uparrow & \Delta & 0 \\ 0 & \Delta^\dagger & -\boldsymbol{t}_\downarrow & -\boldsymbol{\theta}_\downarrow \\ \Delta^\dagger & 0 & -\boldsymbol{\theta}^\dagger_\downarrow & -\boldsymbol{\varepsilon}_\downarrow \end{pmatrix}$$

pairing within bath ↵

pairing between bath & cluster ↵

dSC : simple bath parametrization

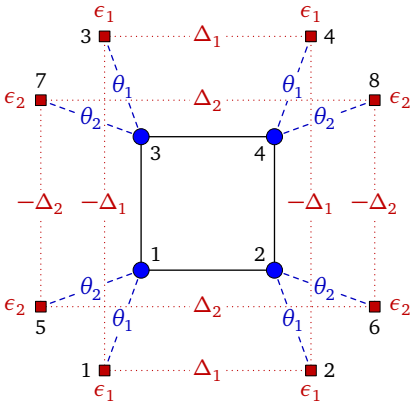

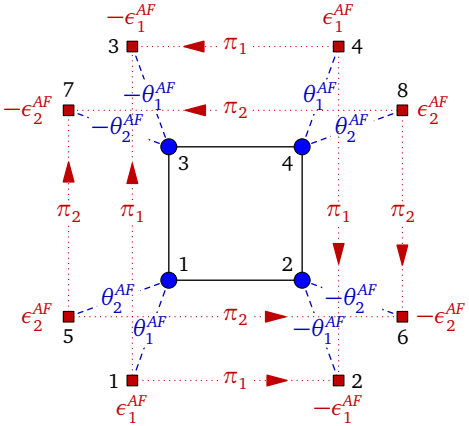

Foley et al., Phys. Rev. B **99** 184510 (2019).

dSC : general parametrization

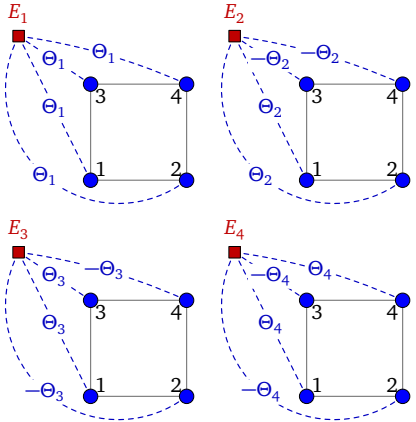

E_i $\pm\Theta_i$ j $\equiv \pm(\theta_i a_i^\dagger c_j + \Delta_i a_i (\mathrm{i}\sigma_y) c_j + \mathrm{H.c.})$

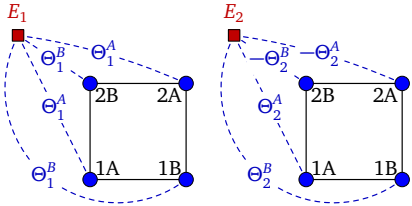

E_i $\pm\Theta_i^X$ jX $\equiv \pm(\theta_{iX} a_i^\dagger c_{jX} + \Delta_{iX} a_i (\mathrm{i}\sigma_y) c_{jX}$
$+\theta_{iX}^s a_i^\dagger \sigma_z c_{jX} + T_{iX} a_i \sigma_x c_{jX} + \mathrm{H.c.})$

Foley et al., Phys. Rev. B **99** 184510 (2019).

dSC : order parameters

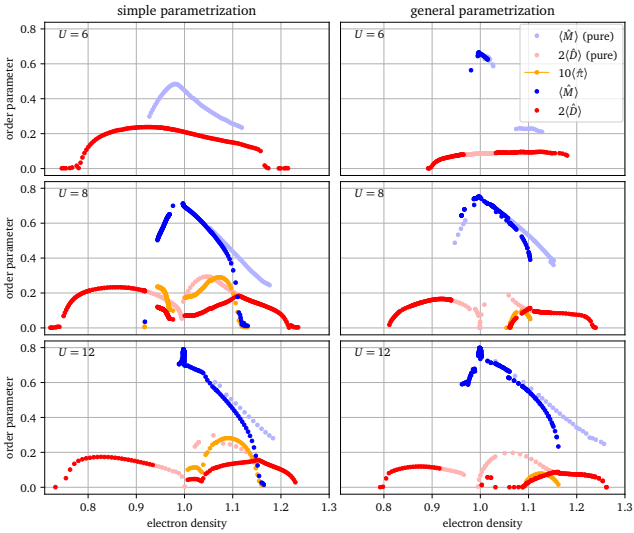

Application: Resilience of dSC to extended interactions

$$H = \sum_{r,r',\sigma} t_{r,r'} c^{\dagger}_{r\sigma} c_{r'\sigma} + U \sum_{r} n_{r\uparrow} n_{r\downarrow} + \sum_{r \neq r'} V_{rr'} n_r n_{r'} - \mu \sum_{r,\sigma} n_{r,\sigma}$$

- Question: effect of NN repulsion V on dSC in the 2D Hubbard model?
  - V is a priori detrimental to dSC (pair breaking effect), and larger than J.
  - But: V increases J.
- Exact treatment of V within the cluster; Hartree approximation between clusters.
- Result: a moderate V has no effect on dSC at low doping.
- The retarded nature of the effective pairing interaction is important.

Resilience of dSC to extended interactions (cont.)

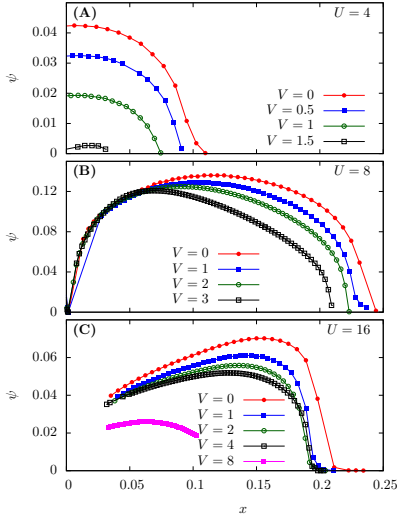

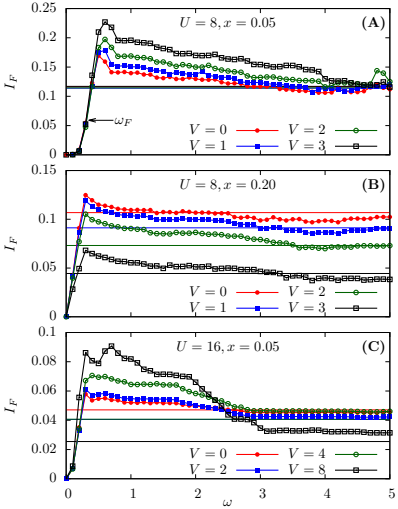

Sénéchal et al., Phys. Rev. B **87**, 075123 (2013).

Non-magnetic impurity in graphene

$$\mathbb{G}^{-1}(\tilde{k},\omega) = \omega - \mathbb{t}(\tilde{k}) - (\omega) = \begin{pmatrix} z - \boldsymbol{t}_{11}(\tilde{k}) - \boldsymbol{\Sigma}_1(\omega) & -\boldsymbol{t}_{12}(\tilde{k}) & -\boldsymbol{t}_{13}(\tilde{k}) & \dots & -\boldsymbol{t}_{1M}(\tilde{k}) \\ -\boldsymbol{t}_{21}(\tilde{k}) & z - \boldsymbol{t}_{22}(\tilde{k}) - \boldsymbol{\Sigma}_2(\omega) & -\boldsymbol{t}_{23}(\tilde{k}) & \dots & -\boldsymbol{t}_{2M}(\tilde{k}) \\ -\boldsymbol{t}_{31}(\tilde{k}) & -\boldsymbol{t}_{32}(\tilde{k}) & z - \boldsymbol{t}_{33}(\tilde{k}) - \boldsymbol{\Sigma}_3(\omega) & \dots & -\boldsymbol{t}_{3M}(\tilde{k}) \\ \vdots & \vdots & \vdots & \ddots & \vdots \\ -\boldsymbol{t}_{M1}(\tilde{k}) & -\boldsymbol{t}_{M2}(\tilde{k}) & -\boldsymbol{t}_{M3}(\tilde{k}) & \dots & z - \boldsymbol{t}_{MM}(\tilde{k}) - \boldsymbol{\Sigma}_M(\omega) \end{pmatrix}$$

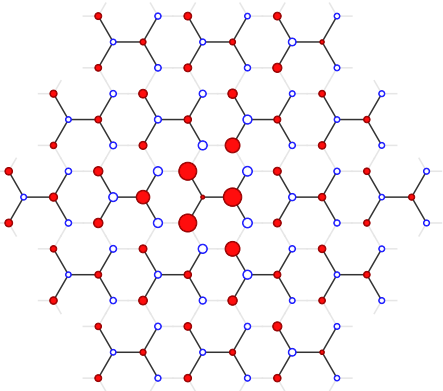

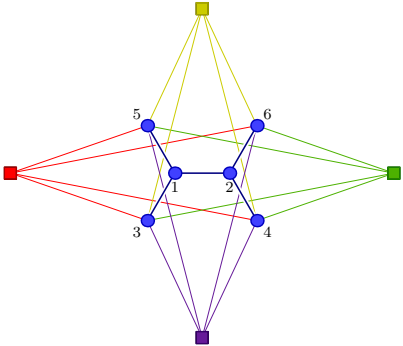

M. Charlebois et al., Phys. Rev. B**91**, 35132 (2015).

Outline

1 Cluster Dynamical Mean Field Theory

2 The impurity solver: Exact Diagonalizations
- Bases and Hamiltonians
- The Lanczos method
- Calculating the Green function
- Cluster symmetries

3 Application to the Emery model

4 PyQCM : a python library for CPT, CDMFT and VCA

5 Advert

Exact diagonalizations vs CT-Quantum Monte Carlo

	ED	**CT-QMC**
temperature	$T = 0$	$T > 0$
frequencies	real/complex	complex + analytic continuation)
sign problem	no	yes
complex HS	yes	no
system size	small	moderate
CDMFT bath	small	infinite
interaction strength	any	depends on expansion scheme

The exact diagonalization procedure

1. Build a basis
2. Construct the Hamiltonian matrix (stored or not)
3. Find the ground state (e.g. by the Lanczos method)
   - Calculate ground state properties (expectation values, etc.)
4. Calculate a representation of the one-body Green function:
   - Continuous-fraction representation
   - Lehmann representation
5. Return to the embedding method (CDMFT)

Building the basis (1)

- Depends on $U(1)$ conservations laws ($N_\uparrow$ and/or $N_\downarrow$)
- Basis of occupation number eigenstates:

$$(c_{1\uparrow}^\dagger)^{n_{1\uparrow}} \cdots (c_{L\uparrow}^\dagger)^{n_{L\uparrow}} (c_{1\downarrow}^\dagger)^{n_{1\downarrow}} \cdots (c_{L\downarrow}^\dagger)^{n_{L\downarrow}} |0\rangle \qquad n_{i\sigma} = 0 \quad \text{or} \quad 1$$

- If no pairing nor spin flip terms:
  - Both $N_\uparrow$ and $N_\downarrow$ are conserved
  - Hilbert space factorizes as $V = V_{N_\uparrow} \otimes V_{N_\downarrow}$
  - dimension:

$$d = d(N_\uparrow) d(N_\downarrow) \qquad d(N_\sigma) = \frac{L!}{N_\sigma!(L - N_\sigma)!}$$

Dimension of the Hilbert space at half-filling

- At half-filling ($N_\uparrow = N_\downarrow = L/2$):

$$d = \left(\frac{L!}{[(L/2)!]^2} \right)^2 \sim 2\frac{4^L}{\pi L}$$

L	dimension
2	4
4	36
6	400
8	4 900
10	63 504
12	853 776
14	11 778 624
16	165 636 900

Two-site cluster: Hamiltonian matrix

- Half-filled, two-site Hubbard model: 4 states
- States and Hamiltonian matrix:

$$
\begin{array}{l}
|01,01\rangle \\
|01,10\rangle \\
|10,01\rangle \\
|10,10\rangle
\end{array}
\begin{pmatrix}
U-2\mu & -t & -t & 0 \\
-t & -2\mu & 0 & -t \\
-t & 0 & -2\mu & -t \\
0 & -t & -t & U-2\mu
\end{pmatrix}
$$

spin ↑ occupation ↵ ↳ spin ↓ occupation

Six-site cluster: Hamiltonian matrix

Sparse matrix structure

400×400

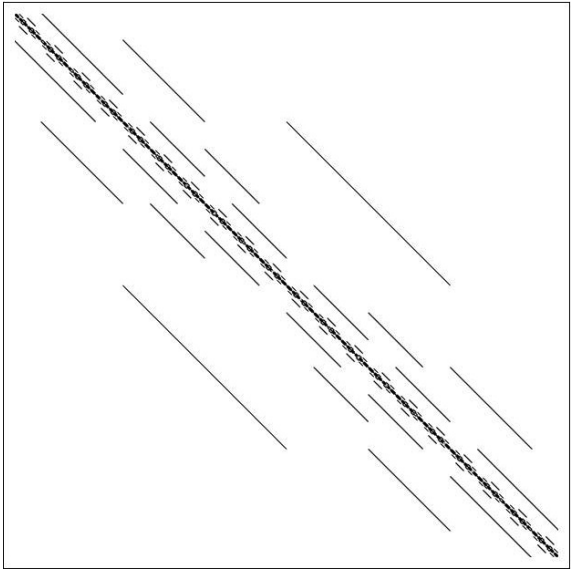

Building the basis (2)

- Basis of occupation number eigenstates:

$$(c_{1\uparrow}^\dagger)^{n_{1\uparrow}} \cdots (c_{L\uparrow}^\dagger)^{n_{L\uparrow}} (c_{1\downarrow}^\dagger)^{n_{1\downarrow}} \cdots (c_{L\downarrow}^\dagger)^{n_{L\downarrow}} |0\rangle \qquad n_{i\sigma} = 0 \quad \text{or} \quad 1$$

- Spin-flip terms but no pairing terms: $N_\uparrow + N_\downarrow$ still conserved.
- Pairing terms but no spin-flip: $N_\uparrow - N_\downarrow$ still conserved.
- Paring terms and spin-flip terms: no $U(1)$ conservation law, dimension 4^L.
- We build a table of binary representations of each state in the basis:

$$b[i] = (n_{1\uparrow}[i] \cdots n_{L\uparrow}[i] n_{1\downarrow}[i] \cdots n_{L\downarrow}[i])_2 = (b_\uparrow[i], b_\downarrow[i])$$

- We find the index from b by binary search

Constructing the Hamiltonian matrix

$$
\begin{aligned}
H_c &= \sum_{\alpha,\beta} t^c_{\alpha\beta} c^\dagger_\alpha c_\beta + \sum_{\alpha,\beta} V^c_{\alpha\beta} n_\alpha n_\beta \\
&= \sum_a h_a H_a
\end{aligned}
$$

- Practical to construct and store (in sparse form) each H_a separately
- For each realization of the impurity model (h_a), one then constructs a single sparse matrix for H
- Matrix elements of Hubbard U : `bit_count(b_up & b_dn)`
- Two basis states $|b\rangle$ and $|b'\rangle$ are connected with $c^\dagger_\alpha c_\beta$ if their binary representations differ at two positions α and β.

$$
\langle b'|c^\dagger_\alpha c_\beta|b\rangle = (-1)^{M_{\alpha\beta}} \qquad M_{\alpha\beta} = \sum_{c=\alpha+1}^{\beta-1} n_c
$$

The Lanczos method

- Problem : Finding the ground state $|\Omega\rangle$ by an iterative application of H
- Start with random vector $|\phi_0\rangle$
- An iterative procedure builds the **Krylov subspace**:

$$\mathscr{K} = \text{span}\left\{|\phi_0\rangle, H|\phi_0\rangle, H^2|\phi_0\rangle, \cdots, H^M|\phi_0\rangle\right\}$$

- The Krylov subspace represents well the extreme (low- and high-) energy sectors of the Hilbert space
- 3-way recursion for an orthogonal basis $\{|\phi_n\rangle\}$:

$$|\phi_{n+1}\rangle = H|\phi_n\rangle - a_n|\phi_n\rangle - b_n^2|\phi_{n-1}\rangle$$

$$a_n = \frac{\langle\phi_n|H|\phi_n\rangle}{\langle\phi_n|\phi_n\rangle} \qquad b_n^2 = \frac{\langle\phi_n|\phi_n\rangle}{\langle\phi_{n-1}|\phi_{n-1}\rangle} \qquad b_0 = 0$$

The Lanczos method (2)

- In the basis of normalized states $|n\rangle = |\phi_n\rangle / \sqrt{\langle \phi_n | \phi_n \rangle}$, the projected Hamiltonian has the tridiagonal form

projector onto $\mathscr{K}$

$$PHP = T = \begin{pmatrix} a_0 & b_1 & 0 & 0 & \cdots & 0 \\ b_1 & a_1 & b_2 & 0 & \cdots & 0 \\ 0 & b_2 & a_2 & b_3 & \cdots & 0 \\ \vdots & \vdots & \vdots & \vdots & \ddots & \vdots \\ 0 & 0 & 0 & 0 & \cdots & a_N \end{pmatrix}$$

- At each step n, find the lowest eigenvalue of that matrix
- Stop when the estimated Ritz residual $\left|\left| T|\psi\rangle - E_0|\psi\rangle \right|\right|$ is small enough
- Run again to find eigenvector $|\psi\rangle = \sum_n \psi_n |n\rangle$ as the $|\phi_n\rangle$'s are not kept in memory.

The Lanczos method: features

- Required number of iterations: typically from 50 to 200
- Extreme eigenvalues converge first
- Rate of convergence increases with separation between ground state and first excited state
- Cannot resolve degenerate ground states : only one state per ground state manifold is picked up
- For degenerate ground states and low lying states (e.g. in DMRG), the Davidson method is generally preferable

The Lanczos method: illustration of the convergence

149 iterations on a matrix of dimension 213,840: eigenvalues of the tridiagonal projection as a function of iteration step

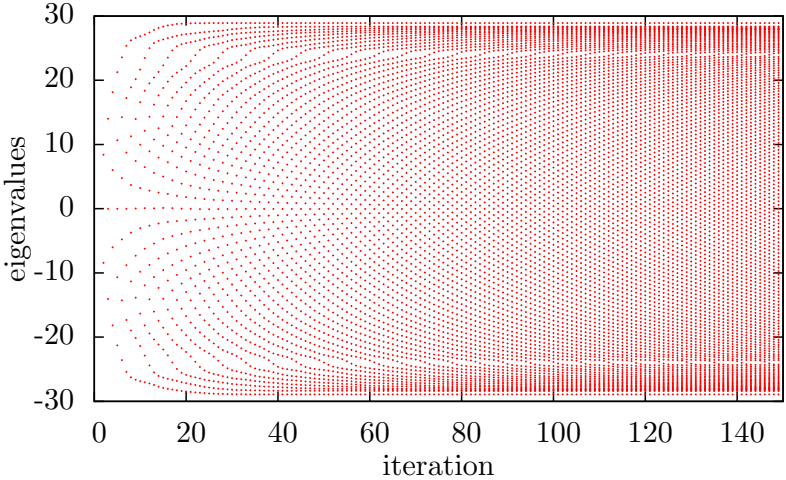

Lanczos method for the Green function

- Zero temperature Green function:

$$G_{\alpha\beta}(z) = G^{(e)}_{\alpha\beta}(z) + G^{(h)}_{\alpha\beta}(z)$$
$$G^{(e)}_{\alpha\beta}(z) = \langle\Omega|c_\alpha \frac{1}{z - H + E_0} c^\dagger_\beta|\Omega\rangle$$
$$G^{(h)}_{\alpha\beta}(z) = \langle\Omega|c^\dagger_\beta \frac{1}{z + H - E_0} c_\alpha|\Omega\rangle$$

- Consider the diagonal element

$$|\phi_\alpha\rangle = c^\dagger_\alpha|\Omega\rangle \implies G^{(e)}_{\alpha\alpha} = \langle\phi_\alpha|\frac{1}{z - H + E_0}|\phi_\alpha\rangle$$

- Perform a Lanczos procedure on $|\phi_\alpha\rangle$.

Lanczos method for the Green function (2)

- Need to find element

$$G^{(e)}_{\alpha\alpha} = \langle \phi_\alpha | \frac{1}{z - PHP + E_0} | \phi_\alpha \rangle$$

- Then $G^{(e)}_{\alpha\alpha}$ is given by a Jacobi continued fraction:

$$G^{(e)}_{\alpha\alpha}(z) = \cfrac{\langle \phi_\alpha | \phi_\alpha \rangle}{z - a_0 - \cfrac{b_1^2}{z - a_1 - \cfrac{b_2^2}{z - a_2 - \cdots}}}$$

- The coefficients a_n and b_n are stored in memory

See, e.g., E. Dagotto, Rev. Mod. Phys. 66:763 (1994)

Lanczos method for the Green function (3)

- What about non diagonal elements $G^{(e)}_{\alpha\beta}$?
- Trick: Define the combination

$$G^{(e)+}_{\alpha\beta}(z) = \langle\Omega|(c_\alpha + c_\beta)\frac{1}{z - H + E_0}(c_\alpha + c_\beta)^\dagger|\Omega\rangle$$

- $G^{(e)+}_{\alpha\beta}(z)$ can be calculated like $G^{(e)}_{\alpha\alpha}(z)$
- Since $G^{(e)}_{\alpha\beta}(z) = G^{(e)}_{\beta\alpha}(z)$, then

$$G^{(e)}_{\alpha\beta}(z) = \frac{1}{2}\left[G^{(e)+}_{\alpha\beta}(z) - G^{(e)}_{\alpha\alpha}(z) - G^{(e)}_{\beta\beta}(z)\right]$$

- Likewise for $G^{(h)}_{\alpha\beta}(z)$

The Lehmann representation

$$G_{\alpha\beta}(z) = \sum_m \frac{\langle\Omega|c_\alpha|m\rangle\langle m|c_\beta^\dagger|\Omega\rangle}{z - E_m + E_0} + \sum_n \frac{\langle\Omega|c_\beta^\dagger|n\rangle\langle n|c_\alpha|\Omega\rangle}{z + E_n - E_0}$$

Define the matrices

$$Q_{\alpha m}^{(e)} = \langle\Omega|c_\alpha|m\rangle \qquad\qquad Q_{\alpha n}^{(h)} = \langle\Omega|c_\alpha^\dagger|n\rangle$$

Then

$$\begin{aligned} G_{\alpha\beta}(z) &= \sum_m \frac{Q_{\alpha m}^{(e)} Q_{\beta m}^{(e)*}}{z - \omega_m^{(e)}} + \sum_n \frac{Q_{\alpha n}^{(h)} Q_{\beta n}^{(h)*}}{z - \omega_n^{(h)}} \\ &= \sum_r \frac{Q_{\alpha r} Q_{\beta r}^*}{z - \omega_r} \qquad\qquad \mathbf{Q}\mathbf{Q}^\dagger = 1 \end{aligned}$$

The Band Lanczos method

- Define $|\phi_\alpha\rangle = c_\alpha^\dagger|\Omega\rangle$, $\alpha = 1, \ldots, L$.
- Extended Krylov space :

$$\left\{|\phi_1\rangle, \ldots, |\phi_L\rangle, H|\phi_1\rangle, \ldots, H|\phi_L\rangle, \ldots, (H)^M|\phi_1\rangle, \ldots, (H)^M|\phi_L\rangle\right\}$$

- States are built iteratively and orthogonalized
- Possible linearly dependent states are eliminated ('deflation')
- A band representation of the Hamiltonian ($2L + 1$ diagonals) is formed in the Krylov subspace.
- It is diagonalized and the eigenpairs are used to build an approximate Lehmann representation

http://www.cs.utk.edu/ dongarra/etemplates/node131.html

Lanczos vs band Lanczos

- The usual Lanczos method for the Green function needs 3 vectors in memory, and $L(L+1)$ distinct Lanczos procedures.
- The band Lanczos method requires $3L+1$ vectors in memory, but requires only 2 iterative procedures ((e) et (h)).
- If Memory allows it, the band Lanczos is much faster.

Cluster symmetries

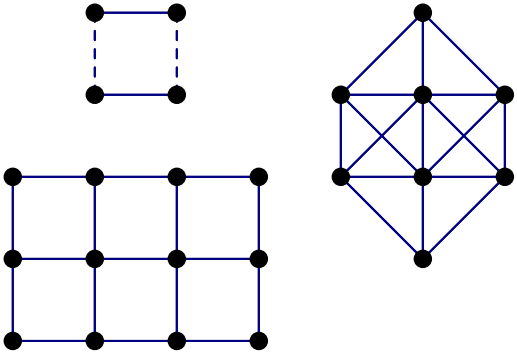

Clusters with C_{2v} symmetry

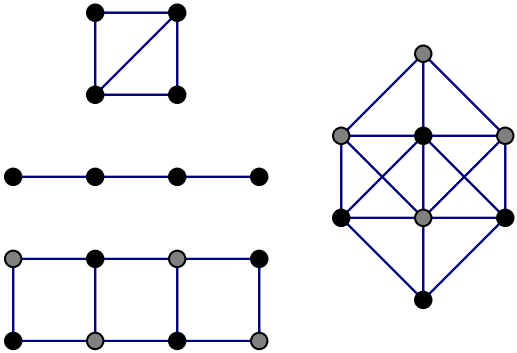

Clusters with C_2 symmetry

Cluster symmetries (2)

- Symmetry operations form a group $\mathfrak{G}$
- The most common occurences are :
  - C_1 : The trivial group (no symmetry)
  - C_2 : The 2-element group (e.g. left-right symmetry)
  - C_{2v} : 2 reflections, 1 π-rotation
  - C_{4v} : 4 reflections, 1 π-rotation, 2 $\pi/2$-rotations
  - C_{3v} : 3 reflections, 3 $2\pi/3$-rotations
  - C_{6v} : 6 reflections, 1 π, 2 $\pi/3$, 2 $\pi/6$ rotations
- States in the Hilbert space fall into a finite number of irreducible representations (irreps) of $\mathfrak{G}$
- The Hamiltonian H' is block diagonal w.r.t. to irreps.
- Easiest to implement with Abelian (i.e. commuting) groups

Taking advantage of cluster symmetries...

order of the group

- Reduces the dimension of the Hilbert space by $\sim |\mathfrak{G}|$
- Accelerates the convergence of the Lanczos algorithm
- Reduces the number of Band Lanczos starting vectors by $|\mathfrak{G}|$
- But: complicates coding of the basis states
- Make use of the projection operator:

dimension of irrep.

$$P^{(\alpha)} = \frac{d_\alpha}{|\mathfrak{G}|} \sum_{g \in \mathfrak{G}} \chi_g^{(\alpha)*} g$$

group character

See, e.g. Poilblanc & Laflorencie cond-mat/0408363

Group characters

C_2	E	C_2
A	1	1
B	1	-1

C_{2v}	e	c_2	σ_1	σ_2
A_1	1	1	1	1
A_2	1	1	-1	-1
B_1	1	-1	1	-1
B_2	1	-1	-1	1

C_{4v}	e	c_2	$2c_4$	$2\sigma_1$	$2\sigma_2$
A_1	1	1	1	1	1
A_2	1	1	1	-1	-1
B_1	1	1	-1	1	-1
B_2	1	1	-1	-1	1
E	2	-2	0	0	0

Taking advantage of cluster symmetries (2)

- Need new basis states, made of sets of binary states related by the group action:

$$|\psi\rangle = \frac{d_\alpha}{|\mathfrak{G}|}\sum_g \chi_g^{(\alpha)*} g|b\rangle \qquad g|b\rangle = \overset{\text{fermionic phase}}{\phi_g(b)}|g\,b\rangle$$

- Then matrix elements take the form

$$\langle\psi_2|H|\psi_1\rangle = \frac{d_\alpha}{|\mathfrak{G}|}\sum_g \chi_h^{(\alpha)*}\phi_g(b)\langle g\,b_2|H|b_1\rangle$$

- When computing the Green function, one needs to use combinations of creation operators that fall into group representations. For instance (4×1):

$$c_1^{(A)} = c_1 + c_4 \qquad c_1^{(B)} = c_1 - c_4$$
$$c_2^{(A)} = c_2 + c_3 \qquad c_2^{(B)} = c_2 - c_3$$

Taking advantage of cluster symmetries (3)

Example : number of matrix elements of the kinetic energy operator (Nearest neighbor) on a 3×4 cluster with C_{2v} symmetry:

dim. value	A_1 213,840	A_2 213,248	B_1 213,440	B_2 213,248
-2	96	736	704	0
$-\sqrt{2}$	12,640	6,208	7,584	5,072
-1	2,983,264	2,936,144	2,884,832	2,911,920
1	952,000	997,168	1,050,432	1,021,392
$\sqrt{2}$	5,088	2,304	3,232	2,992
2	32	0	0	0

Outline

1 Cluster Dynamical Mean Field Theory

2 The impurity solver: Exact Diagonalizations

3 Application to the Emery model

4 PyQCM : a python library for CPT, CDMFT and VCA

5 Advert

Cuprate superconductors

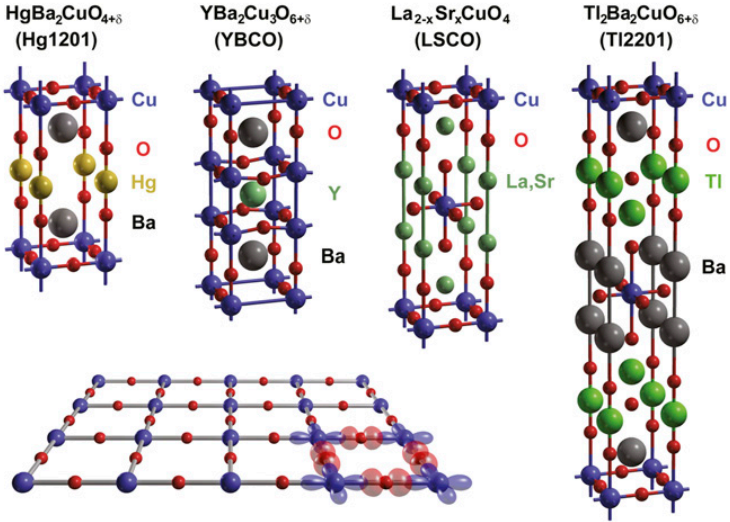

Barišic et al, PNAS **110,** 12235–12240 (2013)

The Emery model (3-band Hubbard model)

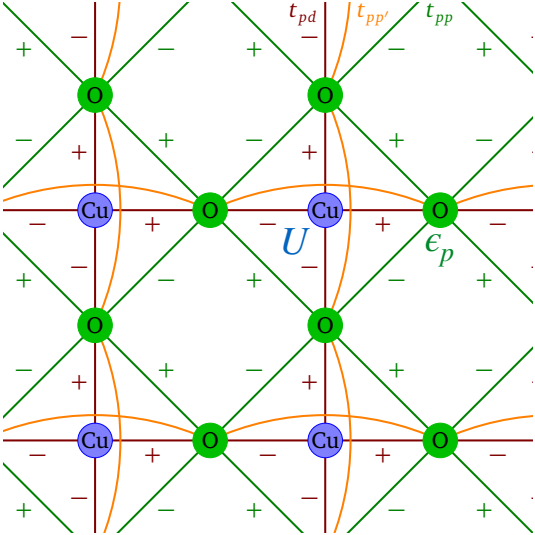

In our version:

U on the Cu orbitals only. Oxygens are uncorrelated.

Parameters: t_{pd} t_{pp} t'_{pp} ϵ_p $U = U_d$

$\epsilon_d = 0$ (reference)

Green function on Copper orbital $G(\mathbf{k}, \omega)$ takes oxygens into account via a hybridization function $\Gamma_O(\mathbf{k}, \omega)$ (nothing to do with the impurity problem):

$$G^{-1}(\mathbf{k}, \omega) = \omega - \epsilon(\mathbf{k}) - \Sigma(\mathbf{k}, \omega) - \Gamma_O(\mathbf{k}, \omega)$$

VJ Emery, Phys. Rev. Lett. 58, 2794 (1987)
CM Varma et al. Solid State Comm. **62** 681 (1987)

Realistic parameters (from LAPW *ab initio* calculations - Wien2K)

	Compound	$\epsilon_d - \epsilon_p$	t_{pd}	t_{pp}	$t_{pp'}$	t'/t	layers	$d^{\text{apical}}_{\text{Cu-O}}$ (Å)	T_c (K)
(1)	La_2CuO_4	2.61	1.39	0.640	0.103	0.070	1	2.3932	38
(2)	$Pb_2Sr_2YCu_3O_8$	2.32	1.30	0.673	0.160	0.108	2	2.3104	70
(3)	$Ca_2CuO_2Cl_2$	2.21	1.27	0.623	0.132	0.085	1	2.7539	26
(4)	$La_2CaCu_2O_6$	2.20	1.31	0.644	0.152	0.120	2	2.2402	45
(5)	$Sr_2Nd_2NbCu_2O_{10}$	2.10	1.25	0.612	0.144	0.110	2	2.0450	28
(6)	$Bi_2Sr_2CuO_6$	2.06	1.36	0.677	0.153	0.105	1	2.5885	24
(7)	$YBa_2Cu_3O_7$	2.05	1.28	0.673	0.150	0.110	2	2.0936	93
(8)	$HgBa_2CaCu_2O_6$	1.93	1.28	0.663	0.187	0.133	2	2.8053	127
(9)	$HgBa_2CuO_4$	1.93	1.25	0.649	0.161	0.122	1	2.7891	90
(10)	$Sr_2CuO_2Cl_2$	1.87	1.15	0.590	0.140	0.108	1	2.8585	30
(11a)	$HgBa_2Ca_2Cu_3O_8$ (outer)	1.87	1.29	0.674	0.184	0.141	3	2.7477	135
(11b)	$HgBa_2Ca_2Cu_3O_8$ (inner)	1.94	1.29	0.656	0.167	0.124	3	2.7477	135
(12)	$Tl_2Ba_2CuO_6$	1.79	1.27	0.630	0.150	0.121	1	2.7143	90
(13)	$LaBa_2Cu_3O_7$	1.77	1.13	0.620	0.188	0.144	2	2.2278	79
(14)	$Bi_2Sr_2CaCu_2O_8$	1.64	1.34	0.647	0.133	0.106	2	2.0033	95
(15)	$Tl_2Ba_2CaCu_2O_8$	1.27	1.29	0.638	0.140	0.131	2	2.0601	110
(16a)	$Bi_2Sr_2Ca_2Cu_3O_{10}$ (outer)	1.24	1.32	0.617	0.159	0.138	3	1.7721	108
(16a)	$Bi_2Sr_2Ca_2Cu_3O_{10}$ (inner)	2.24	1.32	0.678	0.198	0.121	3	1.7721	108

Weber et al., EPL **100** 37001 (2012)

Cartoon density of states (hole picture)

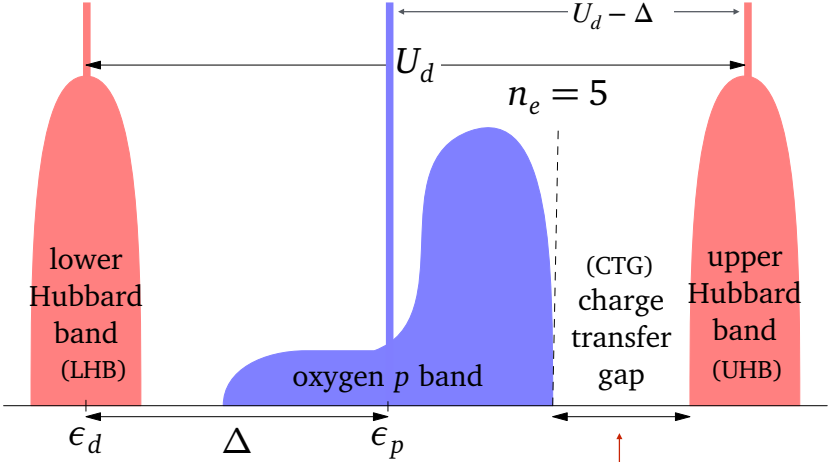

$n_p = 0$

$n_d = 1$

but no so simple…

Dash et al, 10.1103/PhysRevB.100.214509

The Zhang-Rice singlet

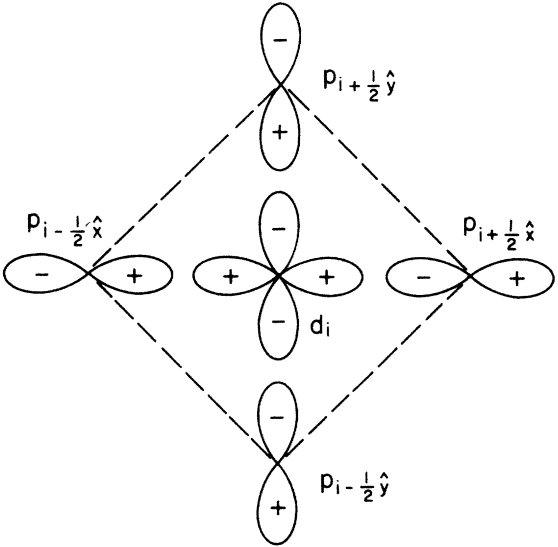

Each copper atom's oxygen neighbor hybridizes with it and forms an almost localized band

FC Zhang & TM Rice, Phys. Rev. B **37**, 3759 (1988)

CDMFT : density of states (**ionic** case)

$t_{pp} = 1$ $t'_{pp} = 1$ $t_{pd} = 1.5$ $\epsilon_p = 7$ $U = 14$

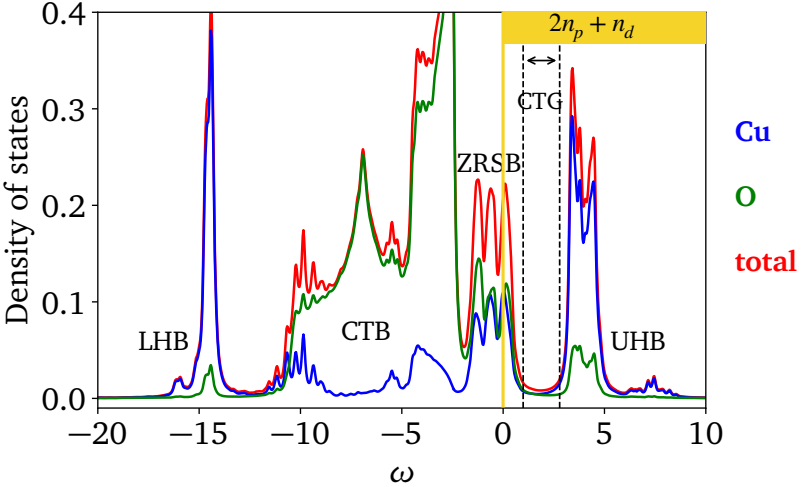

KDST, PNAS **118**, e2106476118 (2021)

CDMFT : density of states (**covalent** case)

$t_{pp} = 1$ $t'_{pp} = 0.2$ $t_{pd} = 2.1$ $\epsilon_p = 2.1$ $U = 14$

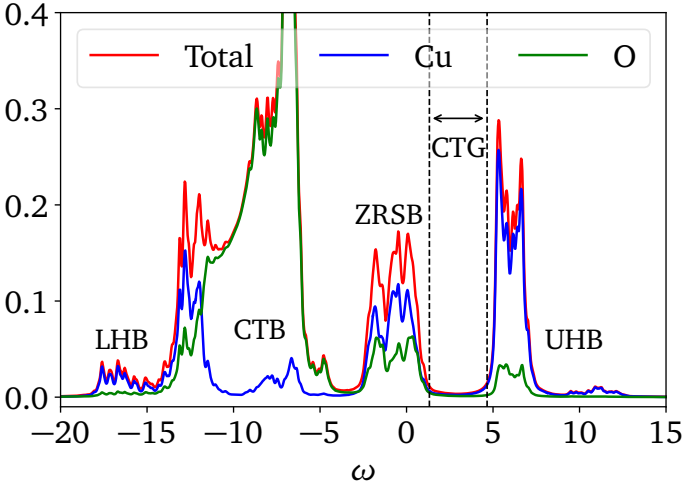

KDST, PNAS **118**, e2106476118 (2021)

Impurity model

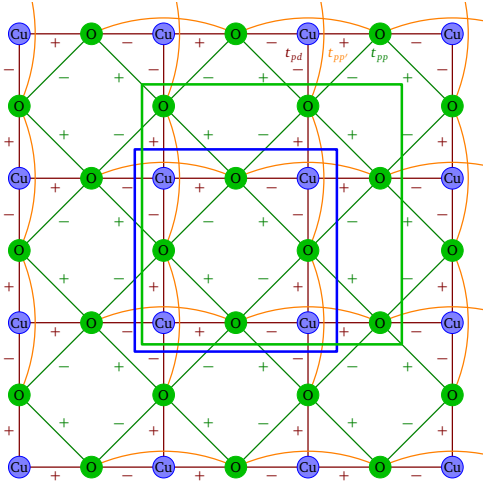

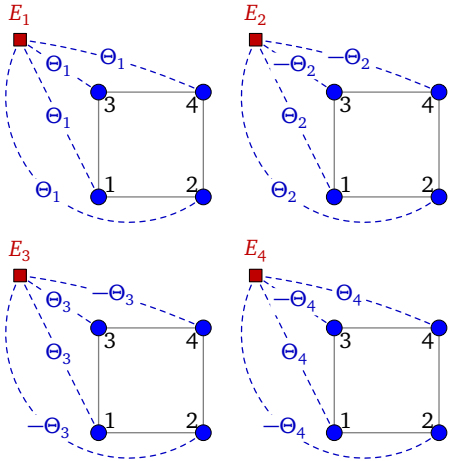

E_i ---- $\pm\Theta_i$ ---- j $\equiv \pm(\theta_i a_i^\dagger c_j + \Delta_i a_i (\mathrm{i}\sigma_y) c_j + \mathrm{H.c.})$

Superconducting order parameter

- ED solver has no sign problem, but stuck at $T = 0$
- Use order parameter as a proxy to T_c

$$2\hat{\Delta} = \sum_{\langle ij \rangle_x} \left(d_{i,\uparrow} d_{j,\downarrow} - d_{i,\downarrow} d_{j,\uparrow} \right) - \sum_{\langle ij \rangle_y} \left(d_{i,\uparrow} d_{j,\downarrow} - d_{i,\downarrow} d_{j,\uparrow} \right) + \mathrm{H.c.}$$

Reduced wave vector

$$\langle \hat{\Delta} \rangle = \oint \frac{d\omega}{2\pi} \frac{d^2\tilde{\mathbf{k}}}{(2\pi)^2} \mathrm{tr} \left[\mathbf{\Delta}(\tilde{\mathbf{k}}) \mathbf{G}(\tilde{\mathbf{k}}, \omega) \right]$$

Average per site

Green function from CDMFT

Oxygen hole content, charge-transfer gap, covalency, and cuprate superconductivity

Nicolas Kowalski[a,b,c], Sidhartha Shankar Dash[a,b,c], Patrick Sémon[a,c], David Sénéchal[a,b,c], and André-Marie Tremblay[a,b,c,1]

[a]Département de physique, Université de Sherbrooke, Sherbrooke, QC J1K 2R1, Canada; [b]Institut quantique, Université de Sherbrooke, Sherbrooke, QC J1K 2R1, Canada; and [c]Regroupement québécois sur les matériaux de pointe, Université de Sherbrooke, Sherbrooke, QC J1K 2R1, Canada

Edited by J. C. Séamus Davis, University of Oxford, Oxford, United Kingdom, and approved August 21, 2021 (received for review April 20, 2021)

PNAS 2021 Vol. 118 No. 40 e2106476118

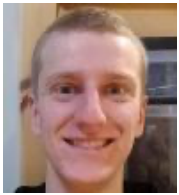



T_c vs oxygen-hole content

experiment # 1

n_p measured by NMR

half-filling : $2n_p + n_d = 1$

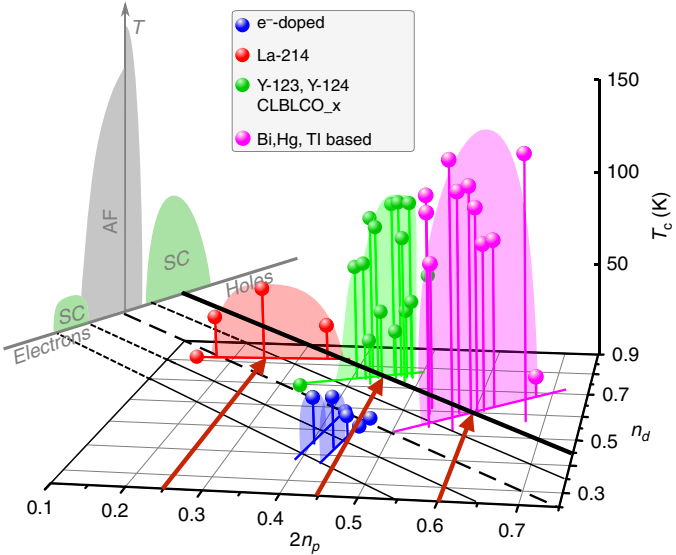

Rybicki et al, Nature comm. **7**, 11413 (2016)

CDMFT : ionic case (CT-QMC)

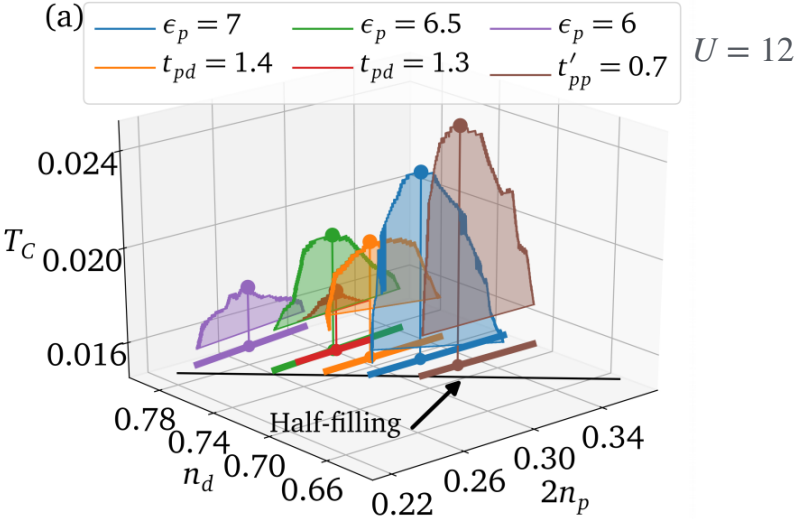

KDST, PNAS **118,** e2106476118 (2021)

Maximum order parameter *vs* $2n_p$

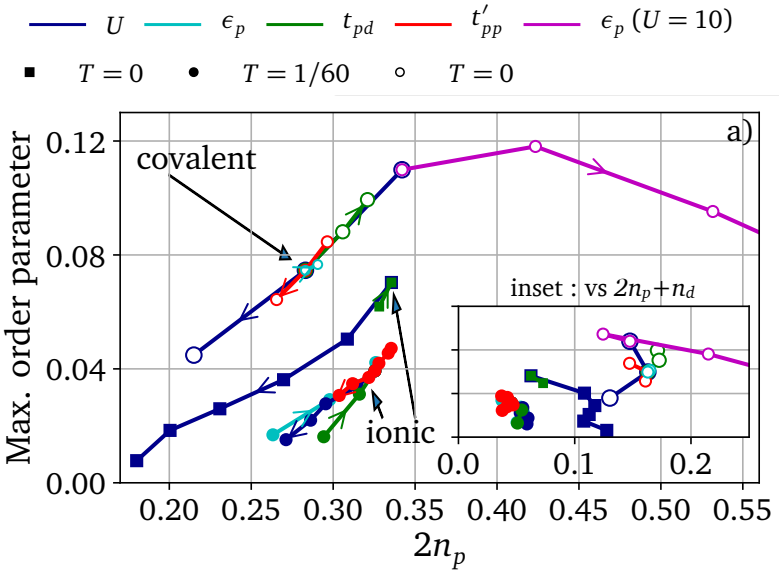

KDST, PNAS **118**, e2106476118 (2021)

CT gap from STM vs superconductivity

experiment # 2

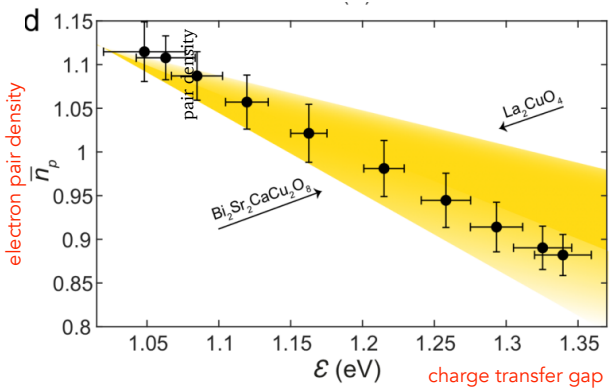

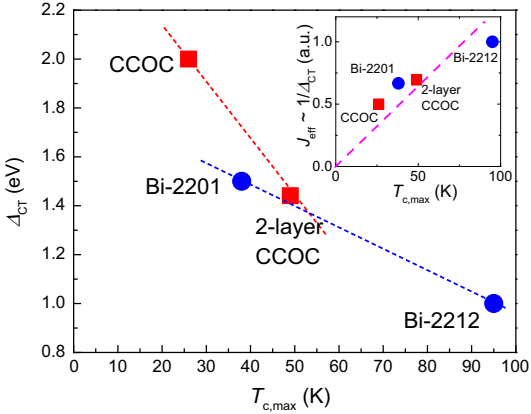

O'Mahony et al, PNAS **119** e2207449119 (2022)

Ruan et al, Sci. Bull. **61**, 1826 (2016)

Optimal n_p *vs* charge transfer gap

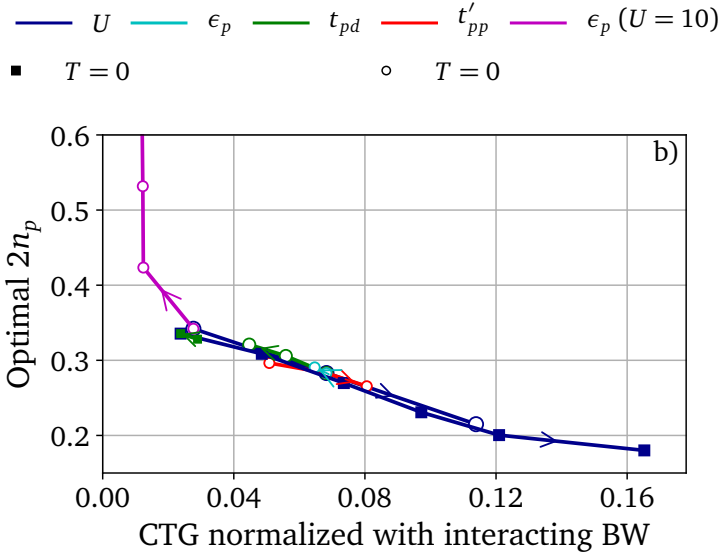

KDST, PNAS **118,** e2106476118 (2021)

Oxygen hole content as witness to CT gap

$\epsilon_p = 7.0, \quad \epsilon_d = 0, \quad t_{pd} = 1.5, \quad t_{pp} = 1.0, \quad t'_{pp} = 1$

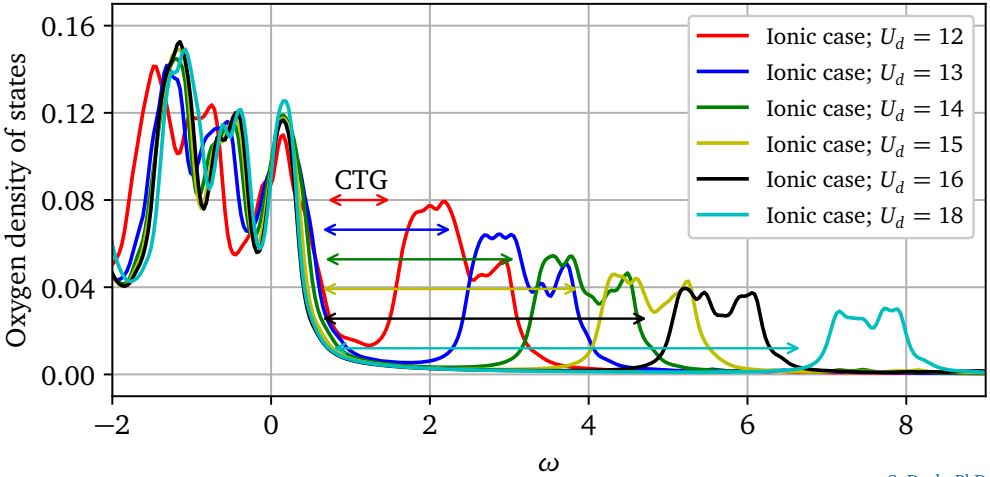

S. Dash, PhD thesis (2021)

Maximum order parameter *vs* CT gap

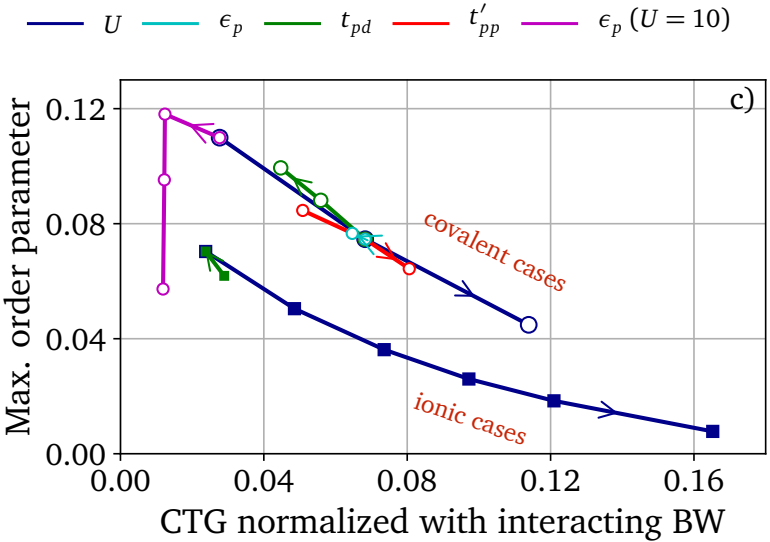

KDST, PNAS **118**, e2106476118 (2021)

T_c *vs* magnetic interaction

- Paramagnon spectra from RIXS. (analog of the isotope effect for magnetic fluctuations)

experiment # 3

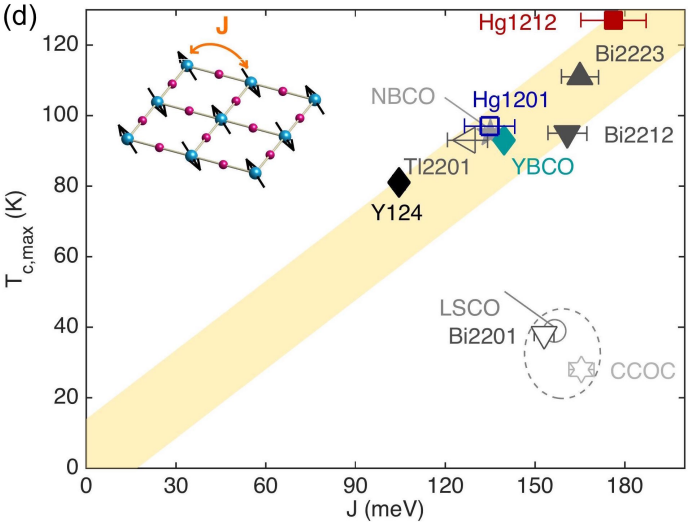

Wang et al, Nature Comm 13:3163 (2022) doi.org/10.1038/s41467-022-30918-z

spin susceptibility and cumulative order parameter

$$I_F(\omega) = -\int_0^{\omega} \frac{d\omega'}{\pi} \mathrm{Im} F_{ij}^R(\omega')$$

$$F(\tau) = -\langle T c_{i\uparrow}(\tau) c_{j\downarrow}(0) \rangle$$

(Gorkov function)

See also:

Kyung *et al*, PRB **80,** 205109 (2009)

Sénéchal *et al*, PRB **87**, 075123 (2013)

Reymbaut *et al*. PRB **94** 155146 (2016)

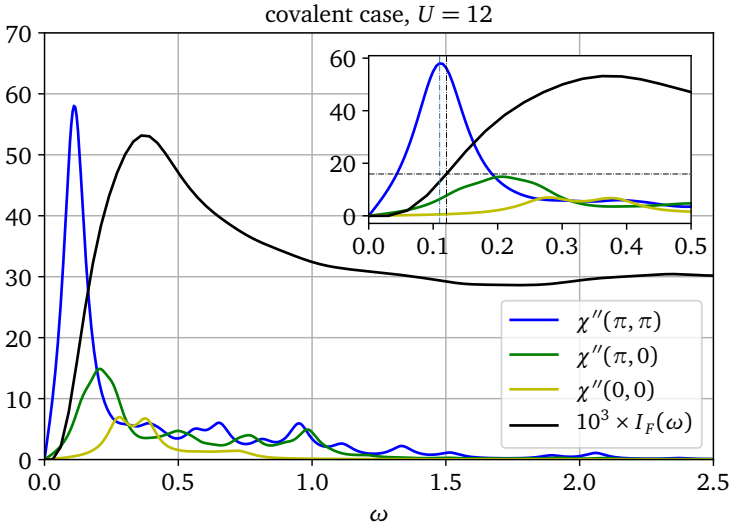

KDST, PNAS **118,** e2106476118 (2021)

cumulative order parameter

$$I_F(\omega) = -\int_0^{\omega} \frac{d\omega'}{\pi} \mathrm{Im} F_{ij}^R(\omega')$$

$I_F(\infty)$ = order parameter

$$F(\tau) = -\langle T c_{i\uparrow}(\tau) c_{j\downarrow}(0) \rangle$$

Gorkov function

$$\chi(\omega) = \langle \Omega | S_z \frac{1}{\omega - H + E_0} S_z | \Omega \rangle + \langle \Omega | S_z \frac{1}{\omega + H - E_0} S_z | \Omega \rangle$$

Effective J vs CT gap

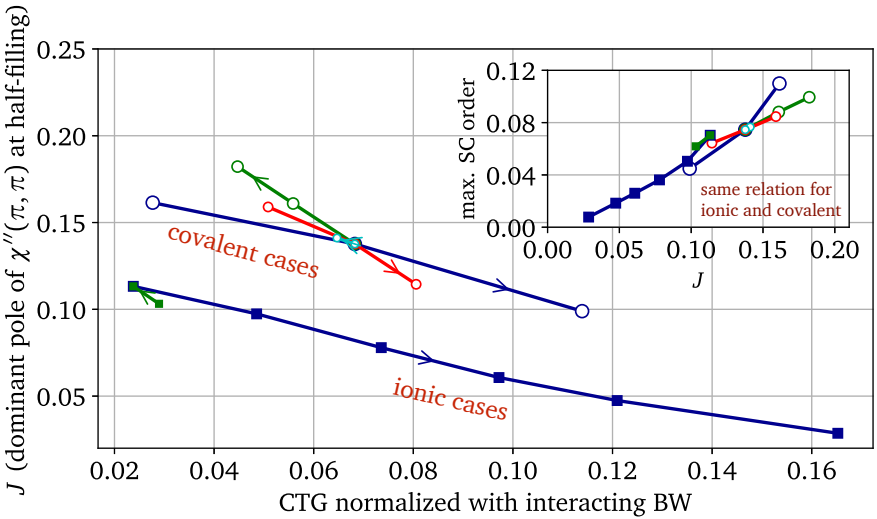

KDST, PNAS **118,** e2106476118 (2021)

Conclusions of this application

- The physics of high-T_c superconductors is well described by a three-band Hubbard model (a.k.a Emery model) at intermediate coupling
- T_c (also the order parameter) at optimal doping is …
  - correlated with the concentration of holes on oxygens
  - anticorrelated with the charge-transfer gap
  - correlated with the superexchange constant J
- This is supported by three types of experiments taken from the litterature (NRM, STM, RIXS)
- Mechanism : short-range AF fluctuations

Quantamagazine

CONDENSED MATTER PHYSICS

High-Temperature Superconductivity Understood at Last

By CHARLIE WOOD September 21, 2022

Outline

1 Cluster Dynamical Mean Field Theory

2 The impurity solver: Exact Diagonalizations

3 Application to the Emery model

4 PyQCM : a python library for CPT, CDMFT and VCA

5 Advert

The PyQCM Library

- C++ core with Python envelope
- CPT, VCA, CDMFT
- High-level stuff (e.g. CDMFT self-consistency loop) in pure Python
- Can simulate most lattice models you can think of, in 0 to 3 dimensions.

SciPost Physics Codebases

Home Authoring Refereeing Submit a manuscript About

Pyqcm: An open-source Python library for quantum cluster methods

Théo N. Dionne, Alexandre Foley, Moïse Rousseau, David Sénéchal

SciPost Phys. Codebases 23 (2023) · published 20 December 2023

doi: 10.21468/SciPostPhysCodeb.23 pdf live repo (external) BiBTeX RIS Submissions/Reports Check for updates

This Publication is part of a bundle

When citing, cite all relevant items (e.g. for a Codebase, cite both the article and the release you used).

DOI	Type
10.21468/SciPostPhysCodeb.23	Article
10.21468/SciPostPhysCodeb.23-r2.2	Codebase release

Outline

1 Cluster Dynamical Mean Field Theory

2 The impurity solver: Exact Diagonalizations

3 Application to the Emery model

4 PyQCM : a python library for CPT, CDMFT and VCA

5 Advert

Advert

Grant from NSERC's Quantum Alliance program:

Realistic electronic structure of correlated quantum materials and quantum devices

in partnership with NANOACADEMIC TECHNOLOGIES

Coherent Modeling

PIs and collaborators :

AM Tremblay (UdeS)

M Côté (UdeM)

M Vergniory (UdeS)

G Kotliar (Rutgers)

D Sénéchal (UdeS)

B Bacq-Labreuil (UdeS)

O Gingras (CCQP)

K Haule (Rutgers)

Objectives

- To create a tool that taps into **DFT** and **DMFT** in order to predict properties of correlated materials and devices
- In particular: to make *material-specific predictions* about superconductivity
- To incorporate these tools into Nanoacademic software, which is tailored for quasi-mesoscopic systems (non-homogenous, thousands of atoms)
- High-throughput simulation of potential new materials

DFT + DMFT

Haule et al, PRB 81, 195107 (2010)

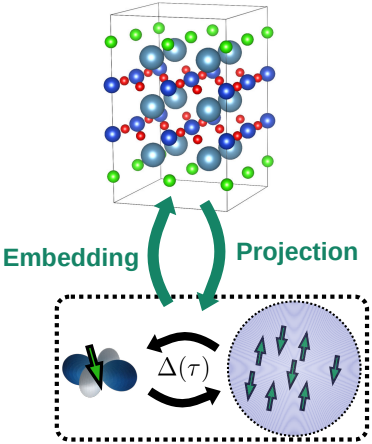

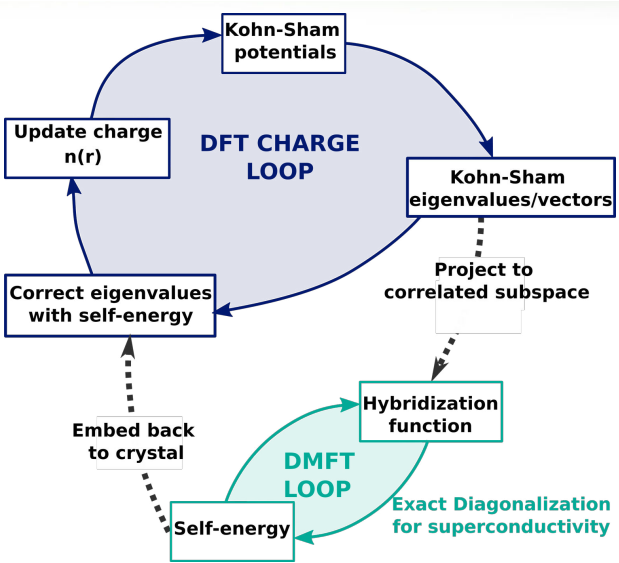

B. Bacq (2024)

Superconducting order parameter (nCCOC & nHBCCO)

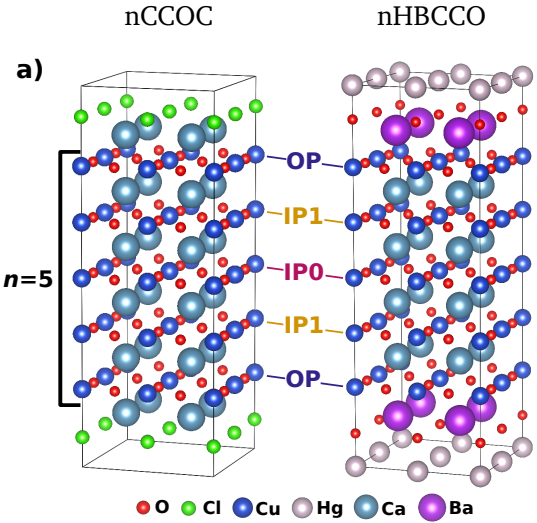

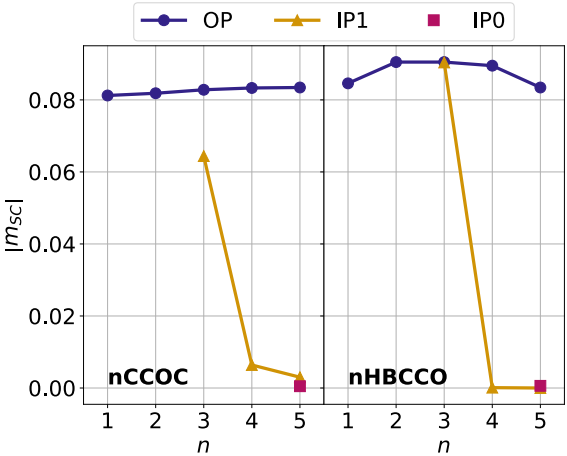

Job advertisement

- **Research assistant / postdoc**
- Up to **5 year** position
- Experience with DFT and/or DMFT
- Ability to work with and adapt existing code (various languages)
- Location : Sherbrooke
- Contact:
  - david.senechal@usherbrooke.ca
  - tremblay@physique.usherbrooke.ca

QUESTIONS ?